

---

# Atomic and Subgraph-aware Bilateral Aggregation for Molecular Representation Learning

---

Jiahao Chen<sup>1,2</sup>, Yurou Liu<sup>1,2</sup>, Jiangmeng Li<sup>3,4</sup>, Bing Su<sup>1,2\*</sup>, Jirong Wen<sup>1,2</sup>

<sup>1</sup>Gaoling School of Artificial Intelligence, Renmin University of China

<sup>2</sup>Beijing Key Laboratory of Big Data Management and Analysis Methods

<sup>3</sup>Institute of Software Chinese Academy of Sciences

<sup>4</sup>University of Chinese Academy of Sciences

{nicelemon666, yurouliu99, subingats}@gmail.com

jiangmeng2019@iscas.ac.cn, jrwen@ruc.edu.cn

## Abstract

Molecular representation learning is a crucial task in predicting molecular properties. Molecules are often modeled as graphs where atoms and chemical bonds are represented as nodes and edges, respectively, and Graph Neural Networks (GNNs) have been commonly utilized to predict atom-related properties, such as reactivity and solubility. However, functional groups (subgraphs) are closely related to some chemical properties of molecules, such as efficacy, and metabolic properties, which cannot be solely determined by individual atoms. In this paper, we introduce a new model for molecular representation learning called the Atomic and Subgraph-aware Bilateral Aggregation (ASBA), which addresses the limitations of previous atom-wise and subgraph-wise models by incorporating both types of information. ASBA consists of two branches, one for atom-wise information and the other for subgraph-wise information. Considering existing atom-wise GNNs cannot properly extract invariant subgraph features, we propose a decomposition-polymerization GNN architecture for the subgraph-wise branch. Furthermore, we propose cooperative node-level and graph-level self-supervised learning strategies for ASBA to improve its generalization. Our method offers a more comprehensive way to learn representations for molecular property prediction and has broad potential in drug and material discovery applications. Extensive experiments have demonstrated the effectiveness of our method.

## 1 Introduction

Molecular representation learning plays a fundamental role in predicting molecular properties, which has broad applications in drug and material discovery [1]. Previous methods typically model molecules as graphs, where atoms and chemical bonds are modeled as nodes and edges, respectively. Therefore, Graph Neural Networks (GNNs) [2] have been widely applied to predict specific properties associated with atoms, such as solubility and reactivity [3–5]. For simplicity, we refer to these models as atom-wise models, as the final molecular representation is the average of each atom.

However, not all molecular properties are determined by individual atoms, and some chemical properties are closely related to functional groups (subgraphs) [5, 6]. For example, a molecule’s efficacy, and metabolic properties are often determined by the functional groups within it. Therefore, many methods propose subgraph-wise models [7, 5], where the final molecular representation is the average of each subgraph. The method proposed in [5] decomposes a given molecule into pieces

---

\*Corresponding author

of subgraphs and learns their representations independently, and then aggregates them to form the final molecular representation. By paying more attention to functional groups, this method ignores the influence of individual atoms<sup>2</sup>, which is harmful to predicting properties related to atoms. More commonly, different properties are sensitive to atoms or functional groups but often determined by both of them at the same time. To verify our point, we do experiments on BBBP and ToxCast dataset and visualize the performance on the test set in Fig. 1 (b) and (c), respectively. It is shown that BBBP is more sensitive to the subgraph-wise branch while Toxcast is the atom-wise branch.

Therefore, both atom-wise and subgraph-wise models have inadequacies and cannot accurately predict current molecular properties independently. To address this dilemma, we propose our Atomic and Subgraph-aware Bilateral Aggregation (ASBA). As shown in Fig. 1 (a), ASBA has two branches, one modeling atom-wise information and the other subgraph-wise information. We follow previous work in constructing the atom-wise branch, which aggregates the representation of each atom and employs a linear classifier to predict properties. For the subgraph-wise branch, we propose a Decomposition-Polymerization GNN architecture where connections among subgraphs are broken in the lower decomposition GNN layers and each subgraph is viewed as a single node in the higher polymerization layers. The decomposition layers serve as a separate GNN module that embeds each subgraph into an embedding, and the relations among subgraphs are modeled by polymerization layers. In this way, the second branch takes subgraphs as basic token units and aggregates them as the final representation. Similar to the atom-wise branch, an independent classifier is added to predict the property. Finally, we incorporate the outputs of the two branches as the prediction score.

In addition, we propose a corresponding self-supervised learning method to jointly pre-train the two branches of our ASBA. Existing self-supervised molecular learning methods mainly design atom-wise perturbation invariance or reconstruction tasks, e.g. predicting randomly masked atoms, but they cannot fully capture subgraph-wise information and the relations among substructures. To this end, we propose a Masked Subgraph-Token Modeling (MSTM) strategy for the subgraph-wise branch. MSTM first tokenizes a given molecule into pieces and forms a subgraph-token dictionary. Compared with atom tokens, such subgraphs correspond to different functional groups, thus their semantics are more stable and consistent. MSTM decomposes each molecule into subgraph tokens, masks a portion of them, and learns the molecular representation by taking the prediction of masked token indexes in the dictionary as the self-supervised task. For the atom-wise branch, we simply employ the masked atom prediction task. Although the atom-wise branch and the subgraph-wise branch aim to extract molecular features from different levels, the global graph representations for the same molecule should be consistent. To build the synergistic interaction between the two branches for joint pre-training, we perform contrastive learning to maximize the consistency of representations between different branches. Experimental results show the effectiveness of our method.

Our contributions can be summarized as:

1. We propose a bilateral aggregation model to encode the characteristics of both atoms and subgraphs with two branches. For the subgraph branch, we propose a novel decomposition-polymerization architecture to embed each subgraph token independently with decomposition layers and polymerize subgraph tokens into the final representation with polymerization layers. In this way, subgraph-level embeddings remain invariant in different molecules, and structural knowledge is explicitly incorporated.
2. We propose a cooperative node-level and graph-level self-supervised learning method to jointly train the two branches of our bilateral model. For the subgraph branch, we propose MSTM, a novel self-supervised molecular learning strategy, which uses the auto-discovered subgraphs as tokens and predicts the dictionary indexes of masked tokens. The subgraph tokens are more stable in function and have more consistent semantics. In this way, masked subgraph modeling can be performed in a principled manner. At the global graph level, we perform a contrastive learning strategy that imposes the interaction of the two branches with the consistency constraint.
3. We provide extensive empirical evaluations to show that the learned representation by our bilateral model and our self-supervised learning method has a stronger generalization ability in various functional group-related molecular property prediction tasks.

---

<sup>2</sup>The representation of each subgraph merges the atom-wise representation by the attention mechanism, but it does not model atom-representation relationships explicitly.

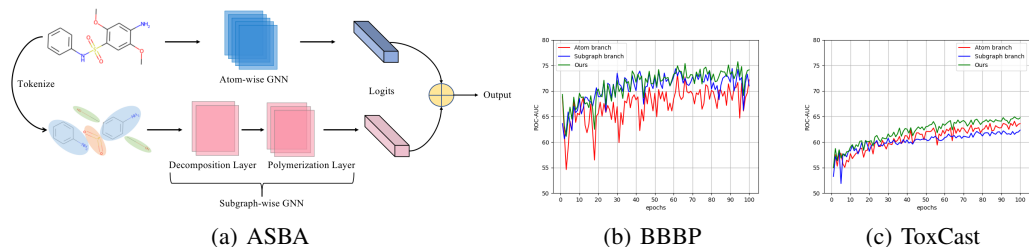


Figure 1: (a) Overview of our ASBA. (b) Testing curves on the BBBP dataset. (c) Testing curves on the ToxCast dataset.

## 2 Related work

**Molecular Property Prediction** The prediction of molecular properties is an important research topic in the fields of chemistry, materials science, pharmacy, biology, physics, etc [8]. Since it is time-consuming and labor-intensive to measure properties via traditional wet experiments, many recent works focus on designing end-to-end machine learning methods to directly predict properties. These works can be divided into two categories: SMILES string-based methods [9, 10] and graph-based methods [11–14]. Compared with SMILES strings, it is more natural to represent molecules as graphs and model them with Graph neural networks (GNNs). However, the training of GNNs requires a large amount of labeled molecule data and supervised-trained GNNs usually show limited generalization ability for newly synthesized molecules and new properties. In order to tackle these issues, self-supervised representation pre-training techniques are explored [15–17] in molecular property prediction.

**Self-supervised Learning of Graphs** Based on how self-supervised tasks are constructed, previous works can be classified into two categories, contrastive models and predictive models. Contrastive models [4, 18–25] generate different views for each graph via data augmentation and learn representations by contrasting the similarities between views of the same graph and different graphs. Predictive models [26, 15, 27] generally mask a part of the graph and predict the masked parts. Most existing methods focus on learning node-level or graph-level representations, with some work involving subgraph-level which utilizes the rich semantic information contained in the subgraphs or motifs. For instance, in [3], the topology information of motifs is considered. In [28], a Transformer architecture is proposed to incorporate motifs and construct 3D heterogeneous molecular graphs for representation learning. Different from these works, we not only propose a bilateral aggregation model with a novel subgraph-aware GNN branch but also propose a joint node-wise and graph-wise self-supervised training strategy so that the learned representation can capture both atom-wise and subgraph-wise information.

## 3 Methodology

### 3.1 Problem formulation

We represent a molecule as a graph  $G = \langle V, E \rangle$  with node attribute vectors  $x_v$  for  $v \in V$  and edge attribute vectors  $e_{uv}$  for  $(u, v) \in E$ , where  $V$  and  $E$  are the sets of atoms and bonds, respectively. We consider a multilabel classification problem with instance  $G$  and label  $\mathbf{y} = \{y_l\}_{l=1}^L$ , where  $y_l \in \{0, 1\}$  denotes whether this property is present in  $G$ . Given a set of training samples  $\mathcal{D}_{train} = \{(G_i, \mathbf{y}_i)\}_{i=1}^{N_1}$ , our target is to learn a mapping  $f : G \rightarrow \mathbb{R}^L$  that can well generalize to the test set. We also have a set of unlabelled support set  $\mathcal{D}_{support} = \{(G_i)\}_{i=1}^{N_2}$ , where  $N_2 \gg N_1$ , and apply our self-supervised learning method to get better initial representation.

### 3.2 Atom-wise branch

Previous works extract the representation of a molecule by aggregating the embeddings of all atoms with GNNs. Similarly, our atom-wise branch applies a single GNN model with  $K$  layers to map each molecule graph into an embedding. Specifically, for  $G = \langle V, E \rangle$ , the input embedding  $\mathbf{h}_v^0$  of the

node  $v \in V$  is initialized by  $\mathbf{x}_v$ , the input embedding at the  $k$ -th layer  $\mathbf{e}_{uv}^k$  of the edge  $(u, v) \in E$  is initialized by  $\mathbf{e}_{uv}$ , and the  $K$  GNN layers iteratively update  $\mathbf{h}_v$  by polymerizing the embeddings of neighboring nodes and edges of  $\hat{v}$ . In the  $k$ -th layer,  $\mathbf{h}_v^{(k)}$  is updated as follows:

$$\mathbf{h}_v^{(k)} = \text{COMBINE}^{(k)}(\mathbf{h}_v^{(k-1)}, \text{AGGREGATE}^{(k)}(\{(\mathbf{h}_v^{(k-1)}, \mathbf{h}_u^{(k-1)}, \mathbf{e}_{uv}^k) : u \in \mathcal{N}(v)\})) \quad (1)$$

where  $\mathbf{h}_v^{(k)}$  denotes the embedding of node  $v$  at the  $k$ -th layer, and  $\mathcal{N}(v)$  represents the neighborhood set of node  $v$ . After  $K$  iterations of aggregation,  $\mathbf{h}_v^{(K)}$  captures the structural information within its  $K$ -hop network neighborhoods. The embedding  $\mathbf{z}_A$  of the graph  $G$  is the average of each node.

$$\mathbf{z}_A = \text{MEAN}(\{\mathbf{h}_v^{(K)} | v \in V\}) \quad (2)$$

Then we add a linear classifier  $\mathbf{z}_A \rightarrow \mathbb{R}^L$ . Formally, atom-wise architecture can be described as learning a mapping  $f : G \rightarrow \mathbb{R}^L$ . The loss function of the atom-wise architecture is:

$$\mathcal{L}_{atom} = \frac{1}{N_1} \sum_{(G, \mathbf{y}) \in \mathcal{D}_{train}} \ell(f(G), \mathbf{y}) \quad (3)$$

### 3.3 Subgraph-wise branch

Atoms are influenced by their surrounding contexts and the semantics of a single atom can change significantly in different environments. Functional groups, which are connected subgraphs composed of coordinated atoms, determine most molecular properties. Our proposed hierarchical Decomposition-Polymerization architecture decouples the representation learning into the subgraph embedding phase, where each molecule is decomposed into subgraphs and an embedding vector is extracted from each subgraph, and the subgraph polymerization phase, where subgraphs are modeled as nodes and their embeddings are updated by polymerizing information from neighboring subgraphs. Finally, the final representation is obtained by combining all subgraph-wise embeddings.

**Subgraph vocabulary construction** Functional groups correspond to special subgraphs, however, pre-defined subgraph vocabularies of hand-crafted functional groups may be incomplete, i.e., not all molecules can be decomposed into disjoint subgraphs in the vocabulary. There exist many decomposition algorithms such as the principle subgraph extraction strategy [6] and breaking retrosynthetically interesting chemical substructures (BRICS) [29]. Generally, we denote a subgraph of the molecule  $G$  by  $S = \langle \hat{V}, \hat{E} \rangle \in G$ , where  $\hat{V}$  is a subset of  $V$  and  $\hat{E}$  is the subset of  $E$  corresponding to  $\hat{V}$ . The target of principle subgraph extraction is to constitute a vocabulary of subgraphs  $\mathbb{V} = \{S_{(1)}, S_{(2)}, \dots, S_{(M)}\}$  that represents the meaningful patterns within molecules, where each unique pattern is associated with an index. Details are discussed in Appendix.

**Subgraph embedding** In this phase, we only focus on learning the embedding of each subgraph by modeling the intra-subgraph interactions. For a molecule  $G = \langle V, E \rangle$ , we decompose it into a set of non-overlapped subgraphs  $\{S_{\pi_1}, S_{\pi_2}, \dots, S_{\pi_T}\}$ , where  $T$  is the number of decomposed subgraphs and  $\pi t$  is the corresponding index of the  $t^{\text{th}}$  decomposed subgraph in the constructed vocabulary  $\mathbb{V}$ . For each subgraph  $S_{\pi t} = \langle \hat{V}_{\pi t}, \hat{E}_{\pi t} \rangle$ , we have  $\hat{V}_{\pi t} \subset V$  and  $\hat{E}_{\pi t} \subset E$ . For each edge  $(u, v)$  in  $E$ , we add it into the inter-subgraph edge set  $\mathcal{E}$  if it satisfies that nodes  $u$  and  $v$  are in different subgraphs. Therefore, we have  $V = \cup \hat{V}_{\pi t}$  and  $E = \cup \hat{E}_{\pi t} \cup \mathcal{E}$ .

We apply a single GNN model with  $K_1$  layers to map each decomposed subgraph into an embedding. GNN depends on the graph connectivity as well as node and edge features to learn an embedding for each node  $v$ . We discard the inter-subgraph edge set  $\mathcal{E}$ , any two subgraphs are disconnected and the information will be detached among subgraphs. This is equivalent to feeding each subgraph  $S_{\pi t}$  into the GNN model individually.

By feeding the molecular graph after discarding all inter-subgraph edges into the GNN model, the embeddings of all atoms in the  $T$  decomposed subgraphs are updated in parallel and the embeddings of all subgraphs can be obtained by adaptive pooling. Compared with previous strategies [4, 3] that directly obtain molecular representations from the context-dependent atom-wise embeddings with all edges, our strategy first extracts subgraph-level embeddings. When a subgraph appears in different molecules, both its atom-wise embeddings and the subgraph embedding remain the same.

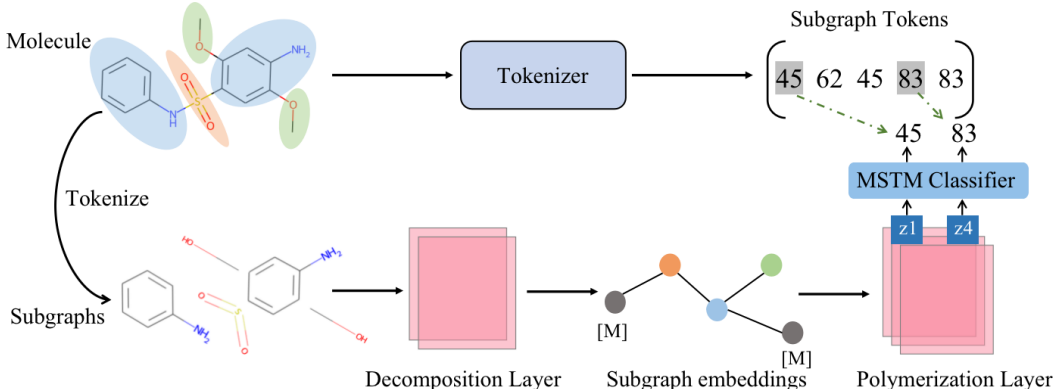


Figure 2: Overview of the MSTM pre-training. We first construct a subgraph vocabulary by automatically mining principle subgraphs from data and each graph in the vocabulary is tokenized. During pre-training, each molecule is decomposed into subgraphs and then fed into the decomposition module, which maps each subgraph into an embedding. Some subgraphs are randomly masked and replaced with a special embedding. These subgraph embeddings are modeled as nodes and further fed into the polymerization module to extract subgraph-level representations. The pre-training task is to predict the masked tokens from the corrupted subgraph-level representations with a linear predictor.

**Subgraph-wise polymerization** In the previous subgraph embedding phase, we view each atom in the subgraph as a node and extract the embedding of each subgraph. In the subgraph-wise polymerization phase, we polymerize the embeddings of neighboring subgraphs for acquiring representations of subgraphs and the final representation of the molecule  $G$ . Differently, we view each subgraph as a node and connect them by the set of inter-subgraph edges  $\mathcal{E}$ . Two subgraphs  $S_{\pi t}$  and  $S_{\pi l}$  are connected if there exists at least one edge  $(\hat{u}, \hat{v}) \in \mathcal{E}$  where  $\hat{u} \in \hat{V}_{\pi t}$  and  $\hat{v} \in \hat{V}_{\pi l}$ . In this way, we construct another graph whose nodes are subgraphs and employ another GNN model with  $K_2$  layers to update the representation of each subgraph and extract the final representation  $\mathbf{z}_S$ . At the  $k'$ -th layer, the embedding  $\mathbf{h}_{\pi t}$  for the  $t$ -th subgraph is updated as follows:

$$\mathbf{h}_{\pi t}^{(k')} = \text{COMBINE}^{(k')}(\mathbf{h}_{\pi t}^{(k'-1)}, \text{AGGREGATE}^{(k')}(\{\mathbf{h}_{\pi t}^{(k'-1)}, \mathbf{h}_{\pi l}^{(k'-1)}, e_{\hat{u}\hat{v}}^{k'} : (\hat{u}, \hat{v}) \in \mathcal{E} \text{ AND } \hat{u} \in \hat{V}_{\pi t} \text{ AND } \hat{v} \in \hat{V}_{\pi l}\})) \quad (4)$$

As shown in Eq.5, representation  $\mathbf{z}_S$  has aggregated all information from different subgraphs, where  $\mathbf{h}_{\pi t}^{(K_2)}$  denotes the subgraph feature which is fed forward after  $K_2$  iterations.

$$\mathbf{z}_S = \text{MEAN}(\{\mathbf{h}_{\pi t}^{(K_2)} | t \in \{1, 2, \dots, k\}\}) \quad (5)$$

The semantics of subgraphs corresponding to functional groups are relatively more stable in different molecular structures. Our polymerization takes such subgraphs as basic units to model the structural interactions and geometric relationships between them. Similarly, we add a linear classifier  $\mathbf{z}_S \rightarrow \mathbb{R}^L$ . Formally, subgraph-wise architecture can be described as learning a mapping  $g : G \rightarrow \mathbb{R}^L$ . The final loss function is:

$$\mathcal{L}_{\text{subgraph}} = \frac{1}{N_1} \sum_{(G, \mathbf{y}) \in \mathcal{D}_{\text{train}}} \ell(g(G), \mathbf{y}) \quad (6)$$

### 3.4 Atomic and Subgraph-aware Bilateral Aggregation (ASBA)

In this section, we propose our ASBA architecture. In the training phase, atom-wise and subgraph-wise branches are trained independently. In the testing phase, since there exists some complementary information between atoms and subgraphs, we aggregate the output of two branches. Formally, the final output is  $(f + g)(G) = (f(G) + g(G))/2$ .

We also give a comprehensive analysis in Sec. 3.6 to explain the superiority of our strategy.

### 3.5 Self-supervised learning

**Node-level self-supervised learning** Many recent works show that self-supervised learning can learn generalizable representations from large unlabelled molecules. Since the atom-wise branch and subgraph-wise branch are decoupled, we can easily apply the existing atom-wise self-supervised learning method to the atom-wise branch of ASBA such as attrMasking [4].

For the subgraph-wise branch, we propose the Masked Subgraph-Token Modeling (MSTM) strategy, which randomly masks some percentage of subgraphs and then predicts the corresponding subgraph tokens. As shown in Fig.2, a training molecule  $G$  is decomposed into  $T$  subgraphs  $\{S_{\pi_1}, S_{\pi_2}, \dots, S_{\pi_T}\}$ . The subgraphs are tokenized to tokens  $\{\pi_1, \pi_2, \dots, \pi_T\}$ , respectively, where  $\pi_t$  is the index of the  $t$ -th subgraph in the vocabulary  $\mathbb{V}$ . Similar to BEiT [30], we randomly mask a number of  $M$  subgraphs and replace them with a learnable embedding. Therefore, we construct a corrupted graph  $\tilde{G}$  and feed it into our hierarchical decomposition-polymerization GNN architecture to acquire polymerized representations of all subgraphs. For each masked subgraph  $\tilde{S}_{\pi_t}$ , we bring an MSTM classifier  $p(\cdot|h_{\pi_t})$  with weight  $\mathbf{W}_p$  and bias  $\mathbf{b}_p$  to predict the ground truth token  $\pi_t$ . Formally, the pre-training objective of MSTM is to minimize the negative log-likelihood of the correct tokens given the corrupted graphs.

$$\mathcal{L}_{MSTM} = \frac{1}{N_2} \sum_{\tilde{G} \in \mathcal{D}_{support}} -\mathbb{E} \left[ \sum_t \log p_{MSTM}(\pi_t | f(\tilde{G})) \right] \quad (7)$$

where  $p_{MSTM}(\pi_t | \tilde{G}) = \text{softmax}(\mathbf{W}_p \tilde{\mathbf{h}}_{\pi_t}^{(K_2)} + \mathbf{b}_p)$ . Different from previous strategies, which randomly mask atoms or edges to predict the attributes, our method randomly masks some subgraphs and predicts their indices in the vocabulary  $\mathbb{V}$  with the proposed decomposition-polymerization architecture. Actually, our prediction task is more difficult since it operates on subgraphs and the size of  $\mathbb{V}$  is larger than the size of atom types. As a result, the learned substructure-aware representation captures high-level semantics of substructures and their interactions and can be better generalized to the combinations of known subgraphs under different scaffolds.

**Graph-level self-supervised learning** Node-level pre-training is not sufficient to acquire generalizable features [31]. Therefore, we propose graph-level self-supervised learning as shown in Eq.8, where  $\mathcal{B}^-$  denotes the negative samples for the anchor sample  $G_i$ .

$$\mathcal{L}_{cl} = \frac{1}{N_2} \sum_{G_i \in \mathcal{D}_{support}} -\log \frac{\exp(\mathbf{z}_{S_i} \cdot \mathbf{z}_{A_i})}{\exp(\mathbf{z}_{S_i} \cdot \mathbf{z}_{A_i}) + \sum_{G_j \in \mathcal{B}^-} \exp(\mathbf{z}_{S_i} \cdot \mathbf{z}_{A_j})} \quad (8)$$

We denote  $\mathbf{z}_A$  and  $\mathbf{z}_S$  as output features of atom-wise and subgraph-wise branches, respectively. The atom-wise branch and subgraph-wise branch focuses on the different viewpoint of the same molecule. Our method maximizes the feature consistency along these two branches and improves the generalization for downstream tasks. In addition, graph-level self-supervised learning makes the two branches interact which can utilize the superiority of our bilateral architecture.

### 3.6 Analysis

In this section, we demonstrate that our ASBA has a lower error bound compared with the single atom-wise branch. For simplicity, we consider the case of 1-dimensional feature space, and the conclusion can also be applied in multi-dimensional feature space [32]. Firstly, we give the upper bound of the Bayes error:

**Theorem 1** For a binary classification problem  $T$ , we denote  $\mu_0, \mu_1$  as the mean vector and  $\Sigma_0, \Sigma_1$  as the covariance matrix. Let  $\Sigma$  be the non-singular, average covariance matrix and  $\Sigma = p(c_1)\Sigma_1 + p(c_2)\Sigma_2$ , where  $P(c_1)$  and  $P(c_2)$  are the prior class probability for class  $c_1$  and  $c_2$ , respectively. Then we provide the upper bound of Bayes error  $\mathcal{R}_T$  [33]:

$$\mathcal{R}_T \leq \frac{2P(c_1)P(c_2)}{1 + P(c_1)P(c_2)\Delta}, \quad \text{where } \Delta = (\mu_1 - \mu_2)^T \Sigma^{-1} (\mu_1 - \mu_2) \quad (9)$$

Based on the analysis in [32], we give the upper bound of the expected error for the atom-wise branch and our ASBA in Theorem 2 and Theorem 3, respectively. Proofs are presented in the appendix.

Table 1: Test ROC-AUC performance of different methods on molecular property classification tasks. AVG represents the average results over all benchmarks. We highlight the best and second-best results with **bold** and *bold*. We report the mean and standard results.

Methods	BACE	BBBP	ClinTox	HIV	MUV	SIDER	Tox21	ToxCast	Avg
Infomax	75.9(1.6)	68.8(0.8)	69.9(3.0)	76.0(0.7)	75.3(2.5)	58.4(0.8)	75.3(0.5)	62.7(0.4)	70.3
AttrMasking	79.3(1.6)	64.3(2.8)	71.8(4.1)	77.2(1.1)	74.7(1.4)	61.0(0.7)	<u>76.7(0.4)</u>	64.2(0.5)	71.1
GraphCL	75.4(1.4)	69.7(0.7)	76.0(2.7)	78.5(1.2)	69.8(2.7)	60.5(0.9)	73.9(0.7)	62.4(0.6)	70.8
AD-GCL	78.5(0.8)	70.0(1.1)	79.8(3.5)	78.3(1.0)	72.3(1.6)	63.3(0.8)	76.5(0.8)	63.1(0.7)	72.7
MGSSL	79.1(0.9)	69.7(0.9)	80.7(2.1)	78.8(1.2)	78.7(1.5)	61.8(0.8)	76.5(0.3)	64.1(0.7)	73.7
GraphLoG	<b>83.5(1.2)</b>	72.5(0.8)	76.7(3.3)	77.8(0.8)	76.0(1.1)	61.2(1.1)	75.7(0.5)	63.5(0.7)	73.4
GraphMVP	81.2(0.9)	<u>72.4(1.6)</u>	77.5(4.2)	77.0(1.2)	75.0(1.0)	<b>63.9(1.2)</b>	74.4(0.2)	63.1(0.4)	73.1
GraphMAE	<u>83.1(0.9)</u>	72.0(0.6)	<b>82.3(1.2)</b>	77.2(1.0)	76.3(2.4)	60.3(1.1)	75.5(0.6)	64.1(0.3)	<u>73.8</u>
ASBA(node)	81.9(0.2)	71.8(3.0)	79.0(2.2)	<b>78.8(0.6)</b>	73.7(3.4)	61.2(0.5)	<b>76.7(0.2)</b>	65.6(0.4)	73.6
ASBA(node+graph)	79.4(2.1)	<b>73.9(0.4)</b>	79.5(1.6)	76.3(0.4)	<b>78.7(1.2)</b>	<u>63.4(0.4)</u>	75.8(0.3)	<b>65.7(0.1)</b>	<b>74.1</b>

**Proposition 1** Given a single classification model  $f$ , we have  $f(c|x) = p(c|x) + \epsilon_{c,f}(x)$ , where  $\epsilon_{c,f}(\cdot)$  is the inherent error associated with classes and models. We define  $\epsilon_{c,f}(x) = \beta_c + \eta_{c,f}(x)$ , where  $\beta_c$  is a constant but  $\eta_{c,f}(\cdot)$  is a function associated with samples.

**Theorem 2** Given a single classification model  $f$ , the upper bound of expected error  $\mathcal{R}_T(f)$  is:

$$\mathcal{R}_T(f) = \mathcal{R}_T + \frac{\sigma_{\eta_{c_1,f}}^2 + \sigma_{\eta_{c_2,f}}^2}{2|\nabla_{x=x^*}p(c_1|x) - \nabla_{x=x^*}p(c_2|x)|} \quad (10)$$

**Theorem 3** Given two classification models  $f$ , and  $g$ , which denote atom-wise branch and subgraph-wise branch respectively, we ensemble the logits as the final output. The upper bound of expected error  $\mathcal{R}_T(f + g)$  is:

$$\mathcal{R}_T(f + g) = \mathcal{R}_T + \frac{\sigma_{\eta_{c_1,f}}^2 + \sigma_{\eta_{c_2,f}}^2 + \sigma_{\eta_{c_1,g}}^2 + \sigma_{\eta_{c_2,g}}^2}{8|\nabla_{x=x^*}p(c_1|x) - \nabla_{x=x^*}p(c_2|x)|} \quad (11)$$

Both  $\mathcal{R}_T(f)$  and  $\mathcal{R}_T(f + g)$  are closely associated with the inherent error  $\eta$ . We give a rational hypothesis that inherent errors of two classification models are bounded and the performance of the atom-wise branch is not much worse than that of the subgraph-wise branch. We can draw the conclusion that ASBA has a lower error bound compared with the atom-wise branch. The proof is presented in the appendix.

**Corollary 1** When satisfying  $-\tau_1 < \eta_{c,f} < \tau_1$  and  $-\tau_2 < \eta_{c,g} < \tau_2$ , i.e., the error of both atom-wise and subgraph-wise models are bounded. If satisfying  $\tau_2 < \sqrt{3}\tau_1$ , the expected error upper bound of  $\mathcal{R}_T(f + g)$  will be smaller than single atom-wise branch expected error upper bound we have  $\mathcal{R}_T(f)$ .

## 4 Experiments

### 4.1 Datasets and experimental setup

**Datasets and Dataset Splittings** We use the ZINC250K dataset [34] for self-supervised pre-training, which is constituted of 250k molecules up to 38 atoms. As for downstream molecular property prediction tasks, we test our methods on 8 classification tasks and 3 regression tasks from MoleculeNet [35]. For classification tasks, we follow the *scaffold-splitting* [36], where molecules are split according to their scaffolds (molecular substructures). The proportion of the number of molecules in the training, validation, and test sets is 80% : 10% : 10%. Following [37], we apply random scaffold splitting to regression tasks, where the proportion of the number of molecules in the training, validation, and test sets is also 80% : 10% : 10%. Following [3, 38], we performed three replicates on each dataset to obtain the mean and standard deviation.

**Model configuration and implemented details** To verify the effectiveness of our ASBA, we do experiments with different molecular fragmentation methods, such as BRICS [29] and the principle

Table 2: Test RMSE performance of different methods on the regression datasets.

Methods	Regression dataset					
	fine-tuning			linear probing		
	FreeSolv	ESOL	Lipo	FreeSolv	ESOL	Lipo
Infomax	3.416(0.928)	1.096(0.116)	0.799(0.047)	4.119(0.974)	1.462(0.076)	0.978(0.076)
EdgePred	3.076(0.585)	1.228(0.073)	0.719(0.013)	3.849(0.950)	2.272(0.213)	1.030(0.024)
Masking	3.040(0.334)	1.326(0.115)	0.724(0.012)	3.646(0.947)	2.100(0.040)	1.063(0.028)
ContextPred	2.890(1.077)	1.077(0.029)	0.722(0.034)	3.141(0.905)	1.349(0.069)	0.969(0.076)
GraphLog	2.961(0.847)	1.249(0.010)	0.780(0.020)	4.174(1.077)	2.335(0.073)	1.104(0.024)
GraphCL	3.149(0.273)	1.540(0.086)	0.777(0.034)	4.014(1.361)	1.835(0.111)	0.945(0.024)
3DInfomax	2.639(0.772)	<b>0.891(0.131)</b>	0.671(0.033)	2.919(0.243)	1.906(0.246)	1.045(0.040)
GraphMVP	2.874(0.756)	1.355(0.038)	0.712(0.025)	<b>2.532(0.247)</b>	1.937(0.147)	0.990(0.024)
ASBA(node)	<b>2.589(0.665)</b>	1.050(0.116)	0.562(0.021)	3.237(0.707)	1.397(0.136)	0.807(0.041)
ASBA(node+graph)	3.089(0.841)	<u>1.042(0.106)</u>	<b>0.546(0.001)</b>	3.318(0.708)	<b>1.296(0.350)</b>	<b>0.692(0.011)</b>

Table 3: Test ROC-AUC performance of different methods on molecular property classification tasks with different tokenization algorithms and model configurations.

Methods	BACE	BBBP	ClinTox	HIV	MUV	SIDER	Tox21	ToxCast	Avg
Atom-wise	71.6(4.5)	68.7(2.5)	57.5(3.8)	75.6(1.4)	73.2(2.5)	57.4(1.1)	74.1(1.4)	62.4(1.0)	67.6
	The principle subgraph, $ \mathbb{V}  = 100, K_1 = 2, K_2 = 3$								
Subgraph-wise	64.4(5.2)	69.4(3.0)	59.2(5.2)	71.7(1.5)	68.3(1.6)	59.1(0.9)	72.6(0.8)	61.3(0.7)	65.8
ASBA	72.2(3.3)	70.6(3.2)	61.1(3.0)	76.1(1.8)	72.8(3.3)	59.8(1.3)	75.1(0.4)	63.7(0.5)	69.0
	The principle subgraph, $ \mathbb{V}  = 100, K_1 = 3, K_2 = 2$								
Subgraph-wise	63.1(7.1)	68.7(2.7)	55.8(6.3)	71.7(1.7)	68.3(4.9)	58.7(1.5)	72.9(0.9)	61.5(0.9)	65.1
ASBA	72.3(2.1)	70.9(2.5)	60.6(4.9)	75.5(1.3)	73.3(2.2)	59.6(0.7)	75.3(0.7)	63.9(0.5)	68.9
	The principle subgraph, $ \mathbb{V}  = 300, K_1 = 2, K_2 = 3$								
Subgraph-wise	66.2(4.5)	63.7(3.2)	59.0(8.5)	74.2(1.6)	68.9(1.9)	61.6(1.8)	73.3(0.9)	60.5(0.5)	65.9
ASBA	71.2(4.1)	66.0(4.4)	59.7(4.7)	77.7(1.7)	72.7(2.9)	61.4(1.0)	75.9(0.4)	63.6(0.8)	68.5
	The principle subgraph, $ \mathbb{V}  = 300, K_1 = 3, K_2 = 2$								
Subgraph-wise	67.3(2.0)	66.5(3.3)	54.7(5.7)	73.8(2.1)	69.7(2.5)	60.8(2.5)	73.7(0.7)	60.8(0.7)	65.9
ASBA	71.8(2.5)	68.9(2.3)	55.9(5.3)	77.4(1.8)	74.7(2.5)	61.0(1.1)	76.4(0.7)	63.7(0.6)	68.7
	BRICS, $K_1 = 2, K_2 = 3$								
Subgraph-wise	71.4(3.9)	66.1(3.5)	51.8(3.7)	75.2(1.8)	70.0(2.0)	56.0(1.5)	74.0(0.8)	64.2(1.1)	66.1
ASBA	74.3(4.5)	69.3(2.8)	55.9(3.1)	76.7(1.6)	75.0(2.1)	58.5(1.5)	76.2(0.5)	64.9(1.2)	68.9
	BRICS, $K_1 = 3, K_2 = 2$								
Subgraph-wise	73.6(3.7)	67.0(1.9)	53.0(5.3)	74.0(1.7)	70.5(1.9)	55.8(1.7)	74.4(1.0)	65.0(0.4)	66.7
ASBA	76.8(3.9)	67.8(3.6)	60.0(3.3)	76.9(1.2)	74.4(2.4)	58.1(1.1)	76.7(0.6)	65.7(0.6)	69.6

subgraph [6]. We also do experiments with different hyper-parameter  $K_1$  and  $K_2$ . For self-supervised learning, we employ experiments with the principle subgraph with vocabulary size  $|\mathbb{V}| = 100$ . We perform the subgraph embedding module and the subgraph-wise polymerization module with a  $K_1 = 2$  layer GIN [39] and a  $K_2 = 3$  layer GIN, respectively. For downstream classification tasks and regression tasks, we mainly follow previous work [4] and [37], respectively. For the pre-training phase, we follow the work [3] to use the Adam optimizer [40] with a learning rate of  $1 \times 10^{-3}$ , and batch size is set to 32.

**Baselines** For classification tasks, we comprehensively evaluated our method against different self-supervised learning methods on molecular graphs, including Infomax [41], AttrMasking [4], ContextPred [4], GraphCL [42], AD-GCL [25], MGSSL [3], GraphLog [43], GraphMVP [38] and GraphMAE [27]. For regression tasks, we compare our method with Infomax [41], EdgePred [2], AttrMasking [4], ContextPred [4], GraphLog [43], GraphCL [42], 3DInfomax [17] and GraphMVP [38]. Among them, 3DInfomax exploits the three-dimensional structure information of molecules, while other methods also do not use knowledge or information other than molecular graphs.

## 4.2 Results and Analysis

**Classification** Tab. 1 presents the results of fine-tuning compared with the baselines on classification tasks. ‘‘ASBA(node)’’ denotes we apply node-level self-supervised learning method on our ASBA while ‘‘ASBA(node+graph)’’ denotes we combine node-level and graph-level self-supervised learning



Table 4: Ablation study of self-supervised learning. We report the performance of two branches with different self-supervised learning methods.

Methods	BACE	BBBP	ClinTox	HIV	MUV	SIDER	Tox21	ToxCast	Avg
Node-level self-supervised learning									
Atom-wise	80.0(0.8)	66.4(2.0)	76.8(5.6)	78.6(0.4)	72.4(0.8)	58.2(0.9)	75.4(0.8)	64.5(0.4)	71.5
Subgraph-wise	74.3(2.8)	72.4(1.1)	63.0(7.1)	74.7(1.4)	70.8(4.1)	62.5(0.8)	75.0(0.2)	63.6(0.6)	69.5
ASBA	81.9(0.2)	71.8(3.0)	79.0(2.2)	78.8(0.6)	73.7(3.4)	61.2(0.5)	76.7(0.2)	65.6(0.4)	73.6
Node-level + Graph-level self-supervised learning									
Atom-wise	76.4(2.5)	68.1(1.9)	79.3(1.4)	76.4(0.4)	76.4(0.3)	59.3(1.1)	74.2(0.4)	64.2(0.2)	71.8
Subgraph-wise	77.8(0.9)	71.9(3.4)	75.8(2.9)	73.4(0.3)	74.8(1.2)	63.8(0.8)	74.5(0.4)	63.3(0.7)	71.9
ASBA	79.4(2.1)	73.9(0.4)	79.5(1.6)	76.3(0.4)	78.7(1.2)	63.4(0.4)	75.8(0.3)	65.7(0.1)	74.1

methods. From the results, we observe that the overall performance of our ‘‘ASBA(node+graph)’’ method is significantly better than all baseline methods, including our ‘‘ASBA(node)’’ method, on most datasets. Among them, AttrMasking and GraphMAE also use masking strategies which operate on atoms and bonds in molecular graphs. Compared with AttrMasking, our node+graph method achieves a significant performance improvement of 9.6%, 7.7%, and 4% on BBBP, ClinTox, and MUV datasets respectively, with an average improvement of 3% on all datasets. Compared with GraphMAE, our method also achieved a universal improvement. Compared with contrastive learning models, our method achieves a significant improvement with an average improvement of 3.8% compared with Infomax, 3.3% compared with GraphCL, 1.4% compared with AD-GCL, and 0.7% compared with GraphLoG. For GraphMVP which combines contrastive and generative methods, our method also has an average improvement of 1%.

**Regression** In Tab. 2, we report evaluation results in regression tasks under the fine-tuning and linear probing protocols for molecular property prediction. Other methods are pre-trained on the large-scale dataset ChEMBL29 [44] containing 2 million molecules, which is 10 times the size of the dataset for pre-training our method. The comparison results show that our method outperforms other methods and achieves the best or second-best performance in five out of six tasks, despite being pre-trained only on a small-scale dataset. This indicates that our method can better learn transferable information about atoms and subgraphs from fewer molecules with higher data-utilization efficiency.

**ASBA can achieve better generalization** In Tab. 3, we compare the performance of our atom-level, subgraph-level, and our ASBA integrated model on different classification tasks. From the experimental results, it can be seen that the atom-level branch performs better than the subgraph-level branch on some datasets, such as BACE, ToxCast, and Tox21, while the subgraph-level branch outperforms on others, such as SIDER and BBBP. This is because the influencing factors of different classification tasks are different, some focus on functional groups, while some focus on the interactions between atoms and chemical bonds. However, no matter how the parameters of the model change, our ASBA always achieves better results than the two separate branches on all datasets since it integrates the strengths of both. These results demonstrate that our ASBA has better generalization. We also visualize the testing curves in Fig. 1 (b) and (c), the aggregation results outperform both atom-wise and subgraph-wise in most epochs.

**The effectiveness of graph-level self-supervised learning in the pre-training stage** From Tab. 1 and Tab. 2, it can be seen that adding graph-level self-supervised learning in the pre-training stage can achieve better results in most tasks. Therefore, we investigate two different pre-training methods in Tab. 4. From the experimental results, it can be seen that pre-training the two branches jointly utilizes two self-supervised learning methods than pre-training the two branches individually (only applying node-level self-supervised learning) in general. For detail, graph-level self-supervised learning can give 0.3% and 2.4% gains for the atom-wise branch and subgraph-wise branch, respectively. The overall performance improved by 0.5%. These results demonstrate the necessity of applying graph-level self-supervised learning, which realizes the interaction between two branches.

## 5 Conclusion

In this paper, we address the limitation that molecular properties are not solely determined by atoms by proposing a novel approach called Atomic and Subgraph-aware Bilateral Aggregation (ASBA). The ASBA model consists of two branches: one for modeling atom-wise information and the other for subgraph-wise information. To improve generalization, we propose a node-level self-supervised learning method called MSTM for the under-explored subgraph-wise branch. Additionally, we introduce a graph-level self-supervised learning method to facilitate interaction between the atom-wise and subgraph-wise branches. Experimental results show the effectiveness of our method.

**Limitation:** It is important to note that we did not conduct self-supervised learning experiments on a larger unlabeled dataset due to resource and time limitations.

## References

- [1] Evan N Feinberg, Debnil Sur, Zhenqin Wu, Brooke E Husic, Huanghao Mai, Yang Li, Saisai Sun, Jianyi Yang, Bharath Ramsundar, and Vijay S Pande. Potentialnet for molecular property prediction. *ACS central science*, 4(11):1520–1530, 2018.
- [2] Will Hamilton, Zhitao Ying, and Jure Leskovec. Inductive representation learning on large graphs. *Advances in neural information processing systems*, 30, 2017.
- [3] Zaixi Zhang, Qi Liu, Hao Wang, Chengqiang Lu, and Chee-Kong Lee. Motif-based graph self-supervised learning for molecular property prediction. *Advances in Neural Information Processing Systems*, 34:15870–15882, 2021.
- [4] Weihua Hu, Bowen Liu, Joseph Gomes, Marinka Zitnik, Percy Liang, Vijay Pande, and Jure Leskovec. Strategies for pre-training graph neural networks. *arXiv preprint arXiv:1905.12265*, 2019.
- [5] Nianzu Yang, Kaipeng Zeng, Qitian Wu, Xiaosong Jia, and Junchi Yan. Learning substructure invariance for out-of-distribution molecular representations. In *Advances in Neural Information Processing Systems*, 2022.
- [6] Xiangzhe Kong, Wenbing Huang, Zhixing Tan, and Yang Liu. Molecule generation by principal subgraph mining and assembling. In *Advances in Neural Information Processing Systems*, 2022.
- [7] Yinghui Jiang, Shuting Jin, Xurui Jin, Xianglu Xiao, Wenfan Wu, Xiangrong Liu, Qiang Zhang, Xiangxiang Zeng, Guang Yang, and Zhangming Niu. Pharmacophoric-constrained heterogeneous graph transformer model for molecular property prediction. *Communications Chemistry*, 6(1):60, 2023.
- [8] Junmei Wang and Tingjun Hou. Application of molecular dynamics simulations in molecular property prediction. 1. density and heat of vaporization. *Journal of chemical theory and computation*, 7(7):2151–2165, 2011.
- [9] Keith T Butler, Daniel W Davies, Hugh Cartwright, Olexandr Isayev, and Aron Walsh. Machine learning for molecular and materials science. *Nature*, 559(7715):547–555, 2018.
- [10] Jie Dong, Ning-Ning Wang, Zhi-Jiang Yao, Lin Zhang, Yan Cheng, Defang Ouyang, Ai-Ping Lu, and Dong-Sheng Cao. Admetlab: a platform for systematic admet evaluation based on a comprehensively collected admet database. *Journal of cheminformatics*, 10(1):1–11, 2018.
- [11] Justin Gilmer, Samuel S Schoenholz, Patrick F Riley, Oriol Vinyals, and George E Dahl. Neural message passing for quantum chemistry. In *International conference on machine learning*, pages 1263–1272. PMLR, 2017.
- [12] Kevin Yang, Kyle Swanson, Wengong Jin, Connor Coley, Philipp Eiden, Hua Gao, Angel Guzman-Perez, Timothy Hopper, Brian Kelley, Miriam Mathea, et al. Analyzing learned molecular representations for property prediction. *Journal of chemical information and modeling*, 59(8):3370–3388, 2019.

- [13] Chengqiang Lu, Qi Liu, Chao Wang, Zhenya Huang, Peize Lin, and Lixin He. Molecular property prediction: A multilevel quantum interactions modeling perspective. In *Proceedings of the AAAI Conference on Artificial Intelligence*, volume 33, pages 1052–1060, 2019.
- [14] Johannes Gasteiger, Janek Groß, and Stephan Günnemann. Directional message passing for molecular graphs. *arXiv preprint arXiv:2003.03123*, 2020.
- [15] Yu Rong, Yatao Bian, Tingyang Xu, Weiyang Xie, Ying Wei, Wenbing Huang, and Junzhou Huang. Self-supervised graph transformer on large-scale molecular data. *Advances in Neural Information Processing Systems*, 33:12559–12571, 2020.
- [16] Pengyong Li, Jun Wang, Yixuan Qiao, Hao Chen, Yihuan Yu, Xiaojun Yao, Peng Gao, Guotong Xie, and Sen Song. An effective self-supervised framework for learning expressive molecular global representations to drug discovery. *Briefings in Bioinformatics*, 22(6):bbab109, 2021.
- [17] Hannes Stärk, Dominique Beaini, Gabriele Corso, Prudencio Tossou, Christian Dallago, Stephan Günnemann, and Pietro Liò. 3d infomax improves gnn for molecular property prediction. In *International Conference on Machine Learning*, pages 20479–20502. PMLR, 2022.
- [18] Shichang Zhang, Ziniu Hu, Arjun Subramonian, and Yizhou Sun. Motif-driven contrastive learning of graph representations. *arXiv preprint arXiv:2012.12533*, 2020.
- [19] Fan-Yun Sun, Jordon Hoffman, Vikas Verma, and Jian Tang. Infograph: Unsupervised and semi-supervised graph-level representation learning via mutual information maximization. In *International Conference on Learning Representations*, 2020.
- [20] Yuning You, Tianlong Chen, Yang Shen, and Zhangyang Wang. Graph contrastive learning automated. In *International Conference on Machine Learning*, pages 12121–12132. PMLR, 2021.
- [21] Mengying Sun, Jing Xing, Huijun Wang, Bin Chen, and Jiayu Zhou. Mocl: Contrastive learning on molecular graphs with multi-level domain knowledge. *arXiv preprint arXiv:2106.04509*, 9, 2021.
- [22] Arjun Subramonian. Motif-driven contrastive learning of graph representations. In *Proceedings of the AAAI Conference on Artificial Intelligence*, volume 35, pages 15980–15981, 2021.
- [23] Jun Xia, Lirong Wu, Jintao Chen, Bozhen Hu, and Stan Z Li. Simgrace: A simple framework for graph contrastive learning without data augmentation. In *Proceedings of the ACM Web Conference 2022*, pages 1070–1079, 2022.
- [24] Sihang Li, Xiang Wang, An Zhang, Yingxin Wu, Xiangnan He, and Tat-Seng Chua. Let invariant rationale discovery inspire graph contrastive learning. In *International Conference on Machine Learning*, pages 13052–13065. PMLR, 2022.
- [25] Susheel Suresh, Pan Li, Cong Hao, and Jennifer Neville. Adversarial graph augmentation to improve graph contrastive learning. *Advances in Neural Information Processing Systems*, 34:15920–15933, 2021.
- [26] Ziniu Hu, Yuxiao Dong, Kuansan Wang, Kai-Wei Chang, and Yizhou Sun. Gpt-gnn: Generative pre-training of graph neural networks. In *Proceedings of the 26th ACM SIGKDD International Conference on Knowledge Discovery & Data Mining*, pages 1857–1867, 2020.
- [27] Zhenyu Hou, Xiao Liu, Yukuo Cen, Yuxiao Dong, Hongxia Yang, Chunjie Wang, and Jie Tang. Graphmae: Self-supervised masked graph autoencoders. In *Proceedings of the 28th ACM SIGKDD Conference on Knowledge Discovery and Data Mining*, pages 594–604, 2022.
- [28] Fang Wu, Dragomir Radev, and Stan Z Li. Molformer: motif-based transformer on 3d heterogeneous molecular graphs. *Rn*, 1:1, 2023.
- [29] Jörg Degen, Christof Wegscheid-Gerlach, Andrea Zaliani, and Matthias Rarey. On the art of compiling and using ‘drug-like’ chemical fragment spaces. *ChemMedChem: Chemistry Enabling Drug Discovery*, 3(10):1503–1507, 2008.

- [30] Hangbo Bao, Li Dong, Songhao Piao, and Furu Wei. Beit: Bert pre-training of image transformers. *arXiv preprint arXiv:2106.08254*, 2021.
- [31] Jun Xia, Chengshuai Zhao, Bozhen Hu, Zhangyang Gao, Cheng Tan, Yue Liu, Siyuan Li, and Stan Z Li. Mole-bert: Rethinking pre-training graph neural networks for molecules. 2023.
- [32] Kagan Tumer. *Linear and order statistics combiners for reliable pattern classification*. The University of Texas at Austin, 1996.
- [33] Anil K Jain, Robert P. W. Duin, and Jianchang Mao. Statistical pattern recognition: A review. *IEEE Transactions on pattern analysis and machine intelligence*, 22(1):4–37, 2000.
- [34] Teague Sterling and John J Irwin. Zinc 15–ligand discovery for everyone. *Journal of chemical information and modeling*, 55(11):2324–2337, 2015.
- [35] Zhenqin Wu, Bharath Ramsundar, Evan N Feinberg, Joseph Gomes, Caleb Geniesse, Aneesh S Pappu, Karl Leswing, and Vijay Pande. Moleculenet: a benchmark for molecular machine learning. *Chemical science*, 9(2):513–530, 2018.
- [36] Bharath Ramsundar, Peter Eastman, Patrick Walters, and Vijay Pande. *Deep learning for the life sciences: applying deep learning to genomics, microscopy, drug discovery, and more*. O’Reilly Media, 2019.
- [37] Han Li, Dan Zhao, and Jianyang Zeng. Kpgt: Knowledge-guided pre-training of graph transformer for molecular property prediction. *arXiv preprint arXiv:2206.03364*, 2022.
- [38] Shengchao Liu, Hanchen Wang, Weiyang Liu, Joan Lasenby, Hongyu Guo, and Jian Tang. Pre-training molecular graph representation with 3d geometry. *arXiv preprint arXiv:2110.07728*, 2021.
- [39] Keyulu Xu Weihua Hu Jure Leskovec and Stefanie Jegelka. How powerful are graph neural networks. *ICLR. Keyulu Xu Weihua Hu Jure Leskovec and Stefanie Jegelka*, 2019.
- [40] Diederik P Kingma and Jimmy Ba. Adam: A method for stochastic optimization. *arXiv preprint arXiv:1412.6980*, 2014.
- [41] Petar Veličković, William Fedus, William L Hamilton, Pietro Liò, Yoshua Bengio, and R Devon Hjelm. Deep graph infomax. *arXiv preprint arXiv:1809.10341*, 2018.
- [42] Yuning You, Tianlong Chen, Yongduo Sui, Ting Chen, Zhangyang Wang, and Yang Shen. Graph contrastive learning with augmentations. *Advances in Neural Information Processing Systems*, 33:5812–5823, 2020.
- [43] Minghao Xu, Hang Wang, Bingbing Ni, Hongyu Guo, and Jian Tang. Self-supervised graph-level representation learning with local and global structure. In *International Conference on Machine Learning*, pages 11548–11558. PMLR, 2021.
- [44] Anna Gaulton, Louisa J Bellis, A Patricia Bento, Jon Chambers, Mark Davies, Anne Hersey, Yvonne Light, Shaun McGlinchey, David Michalovich, Bissan Al-Lazikani, et al. ChEMBL: a large-scale bioactivity database for drug discovery. *Nucleic acids research*, 40(D1):D1100–D1107, 2012.